Renewable Energy 85 (2016) 359–370

Contents lists available at ScienceDirect

Renewable Energy

journal homepage: www.elsevier.com/locate/renene

The impact of land use constraints in multi-objective energy-noise wind farm layout optimization

Sami Yamani Douzi Sorkhabi [a], David A. Romero [a, *], Gary Kai Yan [b], Michelle Dao Gu [c], Joaquin Moran [d], Michael Morgenroth [d], Cristina H. Amon [a]

[a] Department of Mechanical & Industrial Engineering, University of Toronto, Toronto, ON, Canada
[b] Department of Mechanical Engineering, University of British Columbia, Vancouver, BC, Canada
[c] Division of Engineering Science, University of Toronto, Toronto, ON, Canada
[d] Renewable Power Division, Hatch, Ltd., Niagara Falls, ON, Canada

ARTICLE INFO

Article history:
Received 28 November 2014
Received in revised form
27 April 2015
Accepted 11 June 2015
Available online 3 July 2015

Keywords:
Wind energy
Wind farms
Wind farm noise
Optimization
Evolutionary algorithms
Renewable energy

ABSTRACT

Recently the environmental impact of onshore wind farms is receiving major attention from both governments and wind farm designers. As land is more extensively exploited for wind farms, it is more likely for wind turbines to be in proximity with human dwellings, infrastructure (e.g. roads, transmission lines), and natural habitats (e.g. rivers, lakes, forests). This proximity makes significant portions of land unusable for the designers, introducing a set of land-use constraints. In this study, we conduct a constrained and continuous-variable multi-objective optimization that considers energy and noise as its objective functions, based on Jensen's wake model and the ISO-9613-2 noise standard. A stochastic evolutionary algorithm (NSGA-II) solves the optimization problem, while the land-use constraints are handled with static and dynamic penalty functions. Results of this study illustrate the effect of constraint severity and spatial distribution of unusable land on the trade-off between energy generation and noise production.

1. Introduction

In recent decades, electricity generation from wind energy has shown a sustained growth all over the world. In 2012, 44.8 GW of wind energy capacity was installed in the world, which brought the total installed wind capacity to 282.5 GW [1]. This milestone made wind energy account for 3% of world's electricity demand [2]. In 2013, the wind energy market continued to grow, with the United States of America adding 12 GW of wind power generation capacity (under construction), and with Canada adding 1.6 GW of generation capacity [2]. In the European Union, wind energy represented the largest share of new installed capacity among all energy sources [3] during 2013. These statistics indicate a strong global growth in wind energy generation, increasing the associated market for related products and services [2].

Notwithstanding these trends, wind energy still faces difficulties for wide adoption. Recently, the health and environmental impacts of onshore wind farms have become a matter of concern for governments and wind farm designers. Although it is not proven that the noise production of turbines has negative health impact on human beings, a number of jurisdictions have established regulations that limit noise emissions [4–6]. Besides the potential health issues, extensive land exploitation for wind farms increases their interference with natural habitats and causes negative environmental impact [7]. This interference together with the noise production of wind farms reduce the available land for turbine sitting.

Wind farm design can be a lengthy and iterative process, in which the designer has to maximize the energy generation or revenue, while verifying compliance with environmental and safety regulations or restrictions. Most of the researchers in this area have strived to maximize energy or revenue of wind farms [8,9]. However, their studies fail to elucidate the nature of the energy-noise trade-off especially under severe land use constraints. Furthermore, the current approaches are not able to investigate the impact of the extent of land use constraints on the optimization results. Thus, these approaches fail to generalize case-specific layout optimization.

In this work, we study the energy-noise trade-off for the wind farm layout optimization (WFLO) problem while considering a set

* Corresponding author.
E-mail address: d.romero@utoronto.ca (D.A. Romero).

http://dx.doi.org/10.1016/j.renene.2015.06.026
0960-1481/

of land use constraints. In other words, this work aims to maximize the energy generation and minimize the noise production while investigating the sensitivity of this trade-off to land use constraints. To this end, the unconstrained multi-objective energy-noise optimization carried out by Kwong et al. [10,11] is extended to include land use constraints. The optimization is performed using a multi-objective, continuous-variable Genetic Algorithm (GA) [12] based on non-domination sorting (NSGA-II, [13]) and the constraints are handled with penalty functions [14].

2. Literature review

In this section, we discuss previous studies that have proposed models or algorithms for the WFLO problem and, due to our focus on constrained wind farm optimization, we also discuss previous work in constraint handling methods for evolutionary algorithms.

Regarding studies on WFLO problem, two main optimization approaches have been applied successfully, namely (i) heuristics and (ii) mathematical programming methods. First, optimization heuristics have been the most commonly used approach, and both stochastic and deterministic versions have been reported in the literature. Methods such as GA and Particle Swarm Optimization (PSO) [15] are the common stochastic heuristics used for solving WFLO problem [8,9,16,17]. In addition, deterministic heuristics such as Extended Pattern Search (EPS) of Du Pont and Cagan [18] are also used in this context; however, they have not ever been as common as stochastic methods. Most of the studies using heuristic methods considered energy or cost as their objective function, while Şişbot et al. [19] carried out a multi-objective energy-cost GA optimization. Kwong et al. [10,11] considered noise as the second objective function for the first time and solved the unconstrained problem with continuous variable GA. Their study showed that there is a trade-off between energy generation and noise production.

A significant portion of the literature on the WFLO problem has focused on improving the optimization models by including more realistic features of the wind farms. For instance, Kusiak and Song [20] considered minimum turbine proximity constraints, and enforced a closed wind farm boundary, these constraints were converted to a second objective function and handled in a multi-objective fashion. They showed that this multi-objective optimization maximizes energy and satisfies all the constraints by minimizing constraint violation. Réthoré et al. [21] suggested a two stage optimization model that used GA in the first stage and gradient-based sequential linear programming in the second stage. The second stage relied on an improved model that considered a comprehensive cost function and a more detailed wind resource distribution including more wind directions and speed bins. Saavedra-Moreno et al. [22] improved their model by considering the spatial distribution of wind speed instead of using a single speed/direction wind distribution for the whole farm terrain. Furthermore, Serrano-González et al. [23,24] modified their optimization by taking infrastructure costs and wind data uncertainty into account. Besides all these improvements in wind farm modelling, the most important contribution of the most recent studies with heuristic methods is the switch to continuous-variable formulations [20,10,11,25–27]. This is an important step in reducing the probability of converging to sub-optimal solutions caused by the coarseness of the discretization approaches typically used in the literature.

Formulations of the WFLO problem amenable for solution with mathematical programming methods, such as mixed-integer programming (MIP), have also been proposed. Donovan [28,29] introduced MIP for solving the WFLO problem. Fagerfjäll [30] used traditional branch-and-bound together with a heuristic to improve the performance of the optimization algorithm. Although MIP solvers are widely available in operation research software packages, they all have limitations solving non-linear, non-convex problems such as WFLO. Both Donovan and Fagerfjäll tried to address this problem by simplifying their wake model at the expense of losing accuracy. To address this issue, Archer et al. [31] improved the simplified wake model by introducing a wind interference coefficient, while Turner et al. [32] suggested more accurate linear and quadratic wake models that can be solved by MIP solvers. However, the accuracy problem was resolved by Zhang et al. [33], who proposed the first constraint programming (CP) and MIP models that incorporated the non-linearity of the problem. Similar to the WFLO work using heuristics, proponents of MIP models have also neglected the land use constraints associated with practical instances of the WFLO problem. However, the main limitation of MIP models is their dependence on coarsely discretized domains. For example, even in recent MIP studies [32,33], the wind farm domain is typically discretized into 100–400 potential turbine locations, with memory requirements and solution times increasing dramatically for finer discretizations.

Finally, from the common constraints encountered by wind farm designers, those related with land usage regulations have not received enough attention from researchers. However, there are a few exceptions that considered land-related parameters for their optimization. Chowdhury et al. [25–27] included the impact of land configuration and turbine selection in their study and used PSO for optimization. They minimized cost of energy and represented it as a function of land orientation and aspect ratio. Chen et al. [34] incorporated the participation rates of land owners in their cost function, which was minimized by GA. They showed that land owners remittances account for approximately 10 % of the wind farm's operating cost. In spite of these studies, the environmental/regulatory land use constraints such as setbacks from rivers, lakes, roads and human dwellings, have been neglected in previous work and are a matter of concern in our study.

Hence, we close our review of the literature by discussing previous developments in constraint handling for evolutionary optimization algorithms, which is our method of choice in the present work. Constraint handling approaches for multi-objective optimization with evolutionary algorithms have been based on (i) constrained-domination, (ii) non-domination ranking, or (iii) penalty functions. Firstly, on the constrained-domination side, Fonseca et al. [35] modified the binary tournament operation for parent selection in order to handle the constraints, introducing the concept of constraint domination, i.e. an extended Pareto dominance criterion that also considers constraint violations. Deb et al. [13] also used the same approach as Fonseca's with a slight difference in their constrained domination definition. Secondly, Ray et al. [36] introduced an alternative approach for constraint handling, in which they defined three different non-domination rankings based on the objective functions, constraints, and combined objectives and constraints. The solutions with higher ranks are chosen for next generation with the priority given to the solutions with high ranks regarding the third ranking. Finally, penalty functions have remained the most widely used constraint handling approach in the context of evolutionary algorithms. The penalty function approach recasts the problem as an unconstrained one by adding (if minimization, subtracting otherwise) a function of constraint violation to the objective functions. As a result, penalty functions are generally applicable to constrained optimization problems, regardless of the optimization method used to solve the unconstrained problem. Here, we shall use the penalty function approach, in order to take advantage of its simple implementation and general applicability; the latter can be beneficial for future studies that may use alternative optimization methods.

This work applies the Non-Domination Sorting Genetic Algoritm (NSGA-II) to a multi-objective, constrained, continuous-variable formulation of the WFLO problem, without any simplifying linearizations of the energy-noise objective functions, and using penalty functions to handle the optimization constraints.

3. Wind farm modelling

This section follows the discussion presented in previous work by the authors, see Ref. [37] for more details.

3.1. Wake modelling

This work uses the analytical closed-form wake model suggested by Jensen [38] to quantify the aerodynamic interactions between turbines. Jensen's model is based on conservation of momentum inside the wake region and its linear expansion in the direction of the main flow. As Betz's theory [39] indicates, the wind speed right behind the rotor is approximately 1/3 of the free stream speed. Since it is assumed that the wake region expands linearly, the down stream wind speed can then be calculated as,

$$u = u_0\left(1 - \frac{2}{3}\left(\frac{r_r}{r_1}\right)^2\right), \tag{1}$$

where $r_1 = r_r + \alpha x$, and α is the wake decay constant, also known as entrainment constant. The sum of kinetic energy deficits from upstream turbines is used to calculate an effective wind speed at the turbines influenced by multiple wakes. Thus, the effective wind speed at a turbine located inside n wake regions can be expressed as,

$$u = u_0\left[1 - \sqrt{\sum_{i=1}^{n}\left(1 - \frac{u_i}{u_o}\right)^2}\right]. \tag{2}$$

Using the effective wind speed at the turbine's rotor, the power production of a turbine can be calculated with the manufacturer-supplied power curve. However, without loss of generality, this work continues the approach of previous work [37,18,20] approach and calculates the power output as a cubic function of effective wind speed at hub height. The cut-in and cut-off speeds are considered to be 4 m/s and 25 m/s respectively. The rated speed is 15 m/s, for which a power of 1.5 MW is generated.

3.2. Noise modelling

In this study, the noise receptors are considered as the locations where the sound level has to be measured or calculated. In wind farm layout design, all the residences inside or in the neighbourhood of the wind farm are potential noise receptors. According to the ISO-9613-2 standard [40], the equivalent continuous downwind octave-band sound pressure level (SPL) at each noise receptor is calculated for each sound source and all the eight octave bands with nominal mid-band frequencies from 63 Hz to 8 kHz [40], as $L_f = L_W + D_c - A$, where L_W is the octave-band sound power emitted by the source, D_c is the directivity correction for sources that are not omni-directional, A is the octave-band attenuation, and f is a subscript indexing each octave-band frequency.

The sound pressure level calculated for each octave-band frequency has to be converted to an effective SPL. Among several octave-band weightings available for this conversion, A-weighted sound pressure levels [6] are customarily used in wind farm layout design. The equivalent continuous A-weighted downwind sound pressure level at a specific location is calculated based on the summation of each sound source's contribution at each octave band,

$$L_{avg} = 10\log\left(\sum_{i=1}^{n_s}\left(\sum_{j=1}^{8}10^{0.1\left(L_f(i,j)+A_f(j)\right)}\right)\right), \tag{3}$$

where n_s is the number of sound sources, j is the index indicating each of the eight standard octave-band mid-band frequencies, and the $A_f(j)$ are the standard A-weighting coefficients.

The attenuation term (A) is the sum of attenuation effects caused by geometrical divergence, atmospheric absorption, ground effects, sound barriers, and miscellaneous effects. In the present work, it is assumed that the attenuation effects due to sound barriers and miscellaneous effects are negligible. Further details for the calculation procedure are available in the ISO-9613-2 document [40].

3.3. Constraint modelling

In this study, both proximity and land-use (regulatory) constraints are considered during the optimization. The proximity constraint ensures that the distance between any pair of turbines is at least five times their diameter. This constraint prevents the turbines from being affected by the strong turbulence and flow-induced vibration present in the wake regions. On the other hand, the regulatory constraint implies that the turbines are not allowed to be located inside the non-feasible areas of the domain, such as environmental setbacks, lakes, and private properties of non-participating owners.

The examination of the proximity constraint is performed by calculating Euclidean distances between the turbines in Cartesian coordinates. Hence, turbine i with coordinates (x_{ti}, y_{ti}) is violating the proximity constraint if there exists a turbine j with coordinates (x_{tj}, y_{tj}) such that,

$$\sqrt{\left(x_{t_i} - x_{t_j}\right)^2 + \left(y_{t_i} - y_{t_j}\right)^2} < 5D, \tag{4}$$

where D is the turbine rotor diameter. To calculate the amount of constraint violation for an infeasible layout with respect to the proximity constraint, the proximity constraint is considered as the first constraint and a constraint function called g_1 is defined as

$$g_1 = \sum_{i=1}^{n_{prox}-1}\sum_{j=i+1}^{n_{prox}}\left(5D - \sqrt{\left(x_{t_i} - x_{t_j}\right)^2 + \left(y_{t_i} - y_{t_j}\right)^2}\right), \tag{5}$$

where n_{prox} is the total number of turbines violating the proximity constraint in an infeasible layout and $\{(x_{ti}, y_{ti}), (x_{tj}, y_{tj})\}$ are the coordinates of each pair of them that violate this constraint.

The regulatory constraint is inspected by assuming that all the non-feasible areas are in the form of convex polygons. This work uses an approach based on the non-feasible polygon's area to determine whether a turbine is located inside it or not. The main idea is to connect the location of the turbine to the polygon's vertices with lines, such that each adjacent pair of vertices creates a triangle with the turbine's location. If the summation of all the triangles' areas is equal to that of the polygon, the turbine is inside the polygon. Based on this approach, turbine i with coordinates (x_{ti}, y_{ti}) is violating the regulatory constraint if there exists a non-feasible polygon called P_k such that,

$$A_{i_k} - A_{P_k} = 0, \tag{6}$$

where A_P and A_i are the area of the non-feasible polygon and the summation of the areas of the aforementioned triangles, respectively. A_P and A_i are expressed in Eq. (7) and Eq. (8) using the so-called shoelace formula [41],

$$A_{P_k} = \frac{1}{2}\left[\sum_{j=1}^{n}\left|\left(x_{v_j}y_{v_{j+1}} - y_{v_j}x_{v_{j+1}}\right)\right|\right] + \frac{1}{2}\left|\left(x_{v_n}y_{v_1} - y_{v_n}x_{v_1}\right)\right| \tag{7}$$

$$A_{i_k} = \frac{1}{2}\left[\sum_{j=1}^{n}\left|x_{t_i}\left(y_{v_j} - y_{v_{j+1}}\right) + x_{v_j}\left(y_{v_{j+1}} - y_{t_i}\right) + x_{v_{j+1}}\left(y_{t_i} - y_{v_j}\right)\right|\right] + \frac{1}{2}\left|x_{t_i}\left(y_{v_n} - y_{v_1}\right) + x_{v_n}\left(y_{v_1} - y_{t_i}\right) + x_{v_1}\left(y_{t_i} - y_{v_n}\right)\right| \tag{8}$$

where $j \in \{1,2,\cdots,n\}$, n is the number of non-feasible polygon's vertices and (x_{vj}, y_{vj}) are the coordinates of each vertex. Similar to the first constraint, a constraint function called g_2 is defined as the sum of the infeasible turbines' minimum distances to the sides of the non-feasible polygon wherein they are located. The distance of turbine i in a polygon with n sides from its jth side is the height of the triangle created by the two vertices of side j and the location point of turbine i. This height can be calculated by dividing the triangle's area by its base, i.e., side j,

$$d_{i,j} = \frac{\left|x_{t_i}\left(y_{v_j} - y_{v_{j+1}}\right) + x_{v_j}\left(y_{v_{j+1}} - y_{t_i}\right) + x_{v_{j+1}}\left(y_{t_i} - y_{v_j}\right)\right|}{\sqrt{\left(x_{v_j} - x_{v_{j+1}}\right)^2 + \left(y_{v_j} - y_{v_{j+1}}\right)^2}} \tag{9}$$

where $j \in \{1,2,\cdots,n\}$. Finally, g_2 can be defined as,

$$g_2 = \sum_{i=1}^{n_{reg}} \min\{d_{i,1}, d_{i,2}, \cdots, d_{i,n}\} \tag{10}$$

where n_{reg} is the number of turbines violating the regulatory constraint.

4. Optimization model

Before going through the problem's formulation, it is essential to introduce the specific notation used. $\mathbb{T}$ is defined as a set of pairs representing the coordinates of the turbines, i.e.,

$$\mathbb{T} = \left\{\left(x_{t_1}, y_{t_1}\right), \left(x_{t_2}, y_{t_2}\right), \cdots, \left(x_{t_{n_T}}, y_{t_{n_T}}\right)\right\}, \tag{11}$$

where n_T is the number of turbines. Similarly, we define $\mathbb{R}$ to show the coordinates of the noise receptors as

$$\mathbb{R} = \left\{\left(x_{r_1}, y_{r_1}\right), \left(x_{r_2}, y_{r_2}\right), \cdots, \left(x_{r_{n_R}}, y_{r_{n_R}}\right)\right\}, \tag{12}$$

where n_R is the number of noise receptors.

The regulatory constraint is imposed by dividing the domain into n_p convex polygons, which are the members of $\mathbb{P}$,

$$\mathbb{P} = \{P_1, P_2, \cdots, P_{n_p}\}, \tag{13}$$

where each P_i is a set of pairs containing the vertices coordinates of polygon i in counter clockwise order,

$$P_i = \left\{\left(x_{v_1}, y_{v_1}\right), \left(x_{v_2}, y_{v_2}\right) \cdots, \left(x_{v_n}, y_{v_n}\right)\right\}. \tag{14}$$

Due to the regulatory constraints, some of the above mentioned polygons are identified as non-feasible polygons. All the non-feasible polygons are included in $\mathbb{S}$, $\mathbb{S} \subset \mathbb{P}$, defined as

$$\mathbb{S} = \{P_i | P_i \text{ is non} - \text{feasible}\}. \tag{15}$$

After identifying the non-feasible polygons, the feasibility percentage of the wind farm domain is defined as,

$$\phi = \frac{\sum_{i=1}^{n_p} A_{P_i} - \sum_{P_i \in \mathbb{S}} A_{P_i}}{\sum_{i=1}^{n_p} A_{P_i}} \times 100, \tag{16}$$

which specifies the available land percentage in the domain for placing turbines.

Now, the WFLO problem can be defined as,

$$\underset{\mathbb{T}}{\text{minimize}} \left\{-AEP(\mathbb{T}), \max_{\mathbb{R}}(SPL(\mathbb{T}, \mathbb{R}))\right\}, \tag{17}$$

subject to,

$$\sqrt{\left(x_{t_i} - x_{t_j}\right)^2 + \left(y_{t_i} - y_{t_j}\right)^2} \geq 5D, \tag{18}$$

$$\forall\left\{\left(x_{t_i}, y_{t_i}\right), \left(x_{t_j}, y_{t_j}\right)\right\} \subset \mathbb{T}, i,j \in \{1,2,\cdots,n_T\}, i \neq j, \text{ and } A_{i_k} - A_{P_k} > 0, \tag{19}$$

$\forall i \in \{1,2,\cdots,n_T\}$, $\forall P_k \in \mathbb{S}$, where A_{P_k} and A_{i_k} are calculated using Eq. (7) and Eq. (8), respectively.

The objective functions of the problem, Annual Energy Production (AEP) and maximum Sound Pressure Level (SPL) are calculated as,

$$AEP(\mathbb{T}) = \sum_{i=1}^{n_T} \sum_{d \in \mathscr{D}} \frac{1}{3}\left(u_{id,\infty}\left(1 - \sqrt{\sum_{j \in \mathscr{U}_{id}}\left(1 - \frac{u_{ijd}}{u_{id,\infty}}\right)}\right)\right)^3 p_d \tag{20}$$

and

$$SPL(\mathbb{T}, \mathbb{R}) = 10\log\left(\sum_{i=1}^{n_T} \sum_{j=1}^{8} 10^{0.1\left(L_f^{(i,j)}(\mathbb{T},\mathbb{R}) + A_f^{(j)}\right)}\right), \tag{21}$$

where $d \in \mathscr{D}$ is the set of all possible wind states (i.e., the set of all possible wind speed-direction bins), $\mathscr{U}_{id}$ is the set of upstream turbines with respect to turbine i for wind state d, $u_{id,\infty}$ is the free stream wind speed at turbine i for wind state d, u_{ijd} is the wind speed at turbine i affected by the single wake of the upstream turbine j for wind state d, and p_d is the occurrence probability of wind state d.

4.1. Multi-objective genetic algorithm

In this study, the multi-objective WFLO problem is solved with the NSGA-II algorithm. This algorithm carries out the fitness assignment by using the objective values to calculate two metrics, namely non-domination rank and crowding distance. First, the non-domination ranking metric assigns an integer rank to each solution according to the Pareto dominance criterion. According to this criterion, the solutions that are part of the Pareto set will receive a rank value of 1, the solutions that become non-dominated after removing the rank 1 solutions are ranked 2, and by repeating the same process all the solutions will receive a non-domination rank. Second, a crowding distance is given to each solution based on its distance, measured in the objective space, to the closest solution with the same non-domination rank. This metric preserves a certain diversity in the population, which is critical for convergence to the global optima [13]. The following paragraph presents a thorough description of the NSGA-II algorithm in the context of WFLO problem.

In order to solve the WFLO problem, n_{pop} feasible turbine layouts are generated randomly as the initial population, and their corresponding objective functions (energy generation, noise level) are evaluated. Subsequently, each population member is given a rank and crowding distance based on the above mentioned metrics. The parents for the next generation are chosen via binary tournament according to their non-domination rank and crowding distance. Solutions with lower non-domination ranks are preferred and the crowding distance is used as a secondary fitness metric with the purpose of breaking ties in the rank-based comparisons. After the parents are selected, an offspring generation of size n_{off} is created by cross-over and mutation operators. Then, the objective function values of this offspring population are calculated, the amount of constraint violation is determined for each individual, and then it is used to penalize the objective functions according to the constraint handling methods. Afterwards, the offspring and parent populations are merged together and re-evaluated with the fitness assignment metrics to select the population that will survive to the next generation. An elitism operator is implemented by maintaining the best n_{pop} members of the population for the next generation. In addition, an off-line archive of the best solutions prevents us from losing any optimal solution during the optimization process. This problem may occur when elitism is implemented on constant population sizes [42]. The readers are referred to [13] for more details about NSGA-II algorithm and its implementation.

In the present work, a set of numerical experiments were performed with typical instances of the WFLO problem, aimed at determining the set of NSGA-II control parameters that resulted in the best optimization solutions. As a result of these experiments, we set the cross-over and mutation probabilities as 0.95 and 0.05 respectively. The choice of n_{pop} and n_{off} is discussed in Section 5. Convergence of NSGA-II is determined by applying the approach of Deb et al. [13]. This approach monitors the changes in crowding distance for a certain number of generations. An optimization process is converged if the variance of rank 1 solutions' crowding distances is less than 0.005 during the last 100 generations. Furthermore, a limit of 80,000 objective function evaluations is introduced as an additional termination criterion; this limit was set as a proxy to restrict the total runtime required to obtain a solution in a way that would be insensitive to the specific hardware used to run the experiments.

4.2. Constraint handling

In this study, three different constraint handling approaches are implemented. The proximity and the regularity constraints are handled with static, dynamic, and death penalty functions. The following paragraphs discuss these approaches and their implementation in the context of the WFLO problem.

Death penalty is the first approach that we use in this work. It discards each infeasible layout as soon as it is generated and produces another layout randomly. As the second approach, static penalty functions [14] are utilized to penalize the objective functions of the infeasible layouts. The penalized objective functions are defined as,

$$AEP^P(\mathbb{T}) = AEP(\mathbb{T}) + \sum_{i=1}^{n_c} (\max(0, g_i))^2 R_{AEP,i} \tag{22}$$

and

$$SPL^P(\mathbb{T}, \mathbb{R}) = SPL(\mathbb{T}, \mathbb{R}) + \sum_{i=1}^{n_c} (\max(0, g_i))^2 R_{SPL,i}, \tag{23}$$

where AEP^P and SPL^P are the penalized objective functions, n_c is the number of constraints, g_i is the i-th constraint function, $R_{AEP,i}$ is the penalty coefficient for the energy objective function for constraint i, and $R_{SPL,i}$ is the penalty coefficient for the noise objective function and constraint i. As mentioned before, we consider two constraints in this study, i.e., proximity and regulatory constraints. Thus, n_c is equal to 2.

Static penalty functions use a constant penalty coefficient for all the generations. This can cause a deviation from convergence and lead to sub-optimal solution sets, especially in the final generations [14]. The dynamic penalty function, on the other hand, avoids this deviation by implementing penalty coefficients that increase gradually as the optimization progresses to the final stages, i.e.,

$$AEP^P(\mathbb{T}) = AEP(\mathbb{T}) + \sum_{i=1}^{n_c} (\max(0, g_i))^2 \left(\frac{t}{C_{gen}}\right)^2 R_{AEP,i} \tag{24}$$

and

$$SPL^P(\mathbb{T}, \mathbb{R}) = SPL(\mathbb{T}, \mathbb{R}) + \sum_{i=1}^{n_c} (\max(0, g_i))^2 \left(\frac{t}{C_{gen}}\right)^2 R_{SPL,i}, \tag{25}$$

where t is the current generation index and C_{gen} is a normalizing constant, defined later. The generation parameter is squared according to the approach suggested in Ref. [43]. Due to the presence of this parameter, the average amount of penalization performed by the dynamic penalty function is less than that for static penalties.

A set of computational experiments was carried out to determine an appropriate value for the penalty coefficients. To avoid potential convergence issues resulting from performing our study with a single penalty coefficient, two different sets of penalty coefficients were used when applying the static penalty approach. Based on the computational experiments, the penalty coefficients were selected to be two orders of magnitude larger than the average value of the objective functions. Since the values of AEP (GWhr) and SPL (dBA) are in the same order of magnitude (~10^2), the penalty coefficients were then set to 10^4 and 4×10^4. For the dynamic penalty approach, a single value of the penalty coefficient is used, set to 10^4. However, two different values are assigned to the C_{gen} parameter, namely $C_{gen} = n_{gen}$ and $C_{gen} = n_{gen}/2$. These parameter choices result in two different trajectories for the penalty coefficients, i.e., $C_1 = (t/n_{gen})^2 \times 10^4$ and $C_2 = (2\,t/n_{gen})^2 \times 10^4$, in the ranges $0-10^4$ and $0-4 \times 10^4$, respectively. When appropriate, the solutions achieved by these two formulations for both static and dynamic approaches are combined together and the overall best solutions are reported.

After discussing the constraint handling methods applied to this work, it is necessary to investigate their behavior in the context of GA. When a layout is penalized with penalty functions, especially with the static or death penalty approaches, the chance for that layout to be chosen by the parent selection, crossover or elitism operators decreases drastically, and GA is compelled to discard that layout and look for a new, random feasible layout in the domain. This characteristic of the penalty functions results in more exploration, or global search. Nevertheless, the situation is slightly different with dynamic penalty functions. The dynamic penalty term increases gradually from a value close to zero in the initial

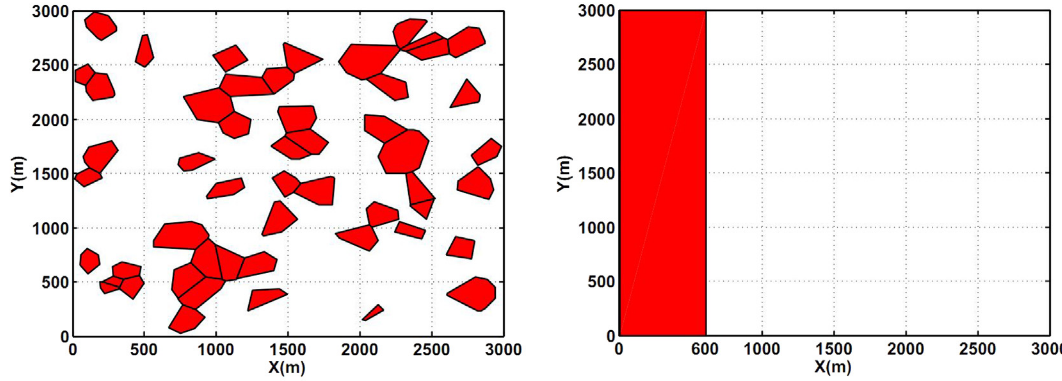

(a) $UP = 0.0469$, $\phi = 80\%$. (b) $UP = 1.0833$, $\phi = 80\%$.

Fig. 1. Uniformity distribution parameter for two sample domains with constant feasibility percentage.

generations to a maximum in the last generation. As a result, the dynamic approach tolerates certain amount of constraint violation. This gives GA the flexibility to use the infeasible layouts as the members of the next generation or as parents. Thus, the GA does not explore the domain to the extent that it does with the static or death penalties, focusing in the areas surrounding the current members of the population during the initial stages. In the final generations, since the penalty term becomes a more dominant value, GA performs a more global search, behaving similarly to the static penalty approach. In other words, the dynamic penalty approach favours local search/exploitation in the initial stages of the optimization and switches to a more global search/exploration later [44–46].

4.3. Spatial distribution of non-feasible land portions

According to preliminary experiments, the percentage of the wind farm land that constitutes the feasible domain, referred herein as feasibility percentage and represented by the symbol ϕ, is not sufficient to quantify the severity of the land use constraints on a given WFLO test case. Although this parameter specifies the unavailable areas for turbine sitting, it does not provide any information about their spatial distribution in the domain. For instance, both Fig. 1(a) and Fig. 1(b) have the same feasibility percentage, i.e., ϕ=80%; however, the spatial distribution of the non-feasible areas are completely different and, as expected, this causes significant differences in the optimization results for the domains in Fig. 1(a) and (b).

Table 1
Wind turbine parameters.

Parameter	Value
Turbine hub height (z)	80 m
Terrain roughness length (z_0)	0.1 m
Rotor radius (r_r)	38.5 m
Thrust coefficient (C_T)	0.8
Power curve	$0.3u^3$ kW
Cut-in speed	4 m/s
Cut-off speed	25 m/s
Rated speed	15 m/s
Rated power	1.5 MW
Noise production (L_w)	100 dB
Noise receptor height (h_r)	1.5 m

Hence, in this study we propose a uniformity parameter to characterize the spatial distribution of the non-feasible areas in the domain, defined in such a way that the more evenly the non-feasible areas are distributed in the domain, the lower its value is. The uniformity parameter (UP) evaluates the distribution uniformity of the non-feasible polygons based on a modification of the Star Discrepancy method [47] suggested by Hickernell et al. [48], which is known as the Centered Discrepancy. This method considers a rectangular domain and measures the uniformity by calculating the discrepancy of normalized center coordinates of each non-feasible polygon with respect to the closest corner point of the domain. The coordinates are normalized by dividing the abscissa and the ordinate of each center by the domain's length and

$$
\begin{aligned}
UP^2 = {} & \left(\frac{13}{12}\right)^2 - \frac{2}{n_p}\sum^{n_p} i = 1\left[1+\frac{1}{2}|x_{c_i}-0.5| - \frac{1}{2}|x_{c_i}-0.5|^2\right] \\
& \left[1+\frac{1}{2}|y_{c_i}-0.5| - \frac{1}{2}|y_{c_i}-0.5|^2\right] \\
& + \frac{1}{n_p^2}\sum^{n_p} i = 1\sum^{n_p} j = 1\left[1+\frac{1}{2}|x_{c_i}-0.5| + \frac{1}{2}|x_{c_j}-0.5| - \frac{1}{2}|x_{c_i}-x_{c_j}|\right] \\
& \left[1+\frac{1}{2}|y_{c_i}-0.5| + \frac{1}{2}|y_{c_j}-0.5| - \frac{1}{2}|y_{c_i}-y_{c_j}|\right].
\end{aligned}
\tag{26}
$$

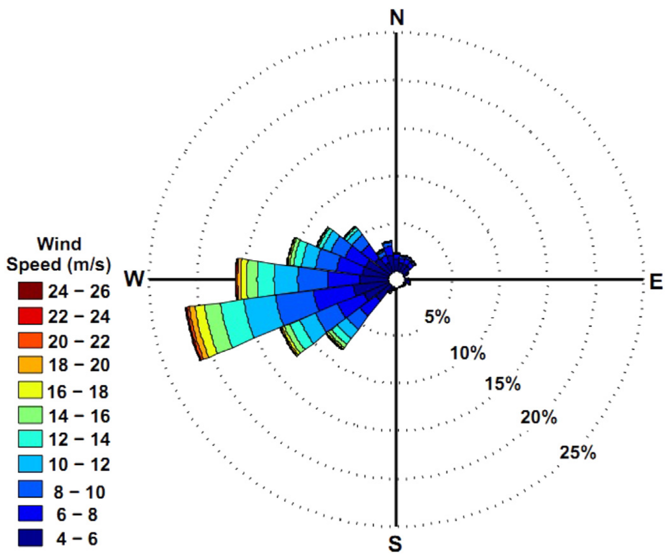

Fig. 2. Wind rose showing the distribution of speed-direction probabilities.

width respectively. The uniformity parameter, which is known as centered discrepancy in the literature has a formula for computation as follows,

In this formulation, (x_{c_i}, y_{c_i}) are the normalized coordinates of the ith non-feasible polygon's center. A detailed discussion about discrepancy methods for uniformity measurement is available in Ref. [49].

5. Test cases

Following the standard test cases found in the wind farm optimization literature, a 3 km $\times$ 3 km square is considered, with turbine and the wind farm terrain characteristics as shown in Table 1. For the wind resource, this work implements the distribution defined by Kusiak et al. [20], which utilizes 24 wind directions in 15° intervals and 43 wind speeds from 4 m/s to 25 m/s in 0.5 m/s intervals. Each direction-speed is assigned a probability based on industrial data, which is used for calculating AEP in Eq. (20). Fig. 2 shows the distribution of the direction-speed probabilities.

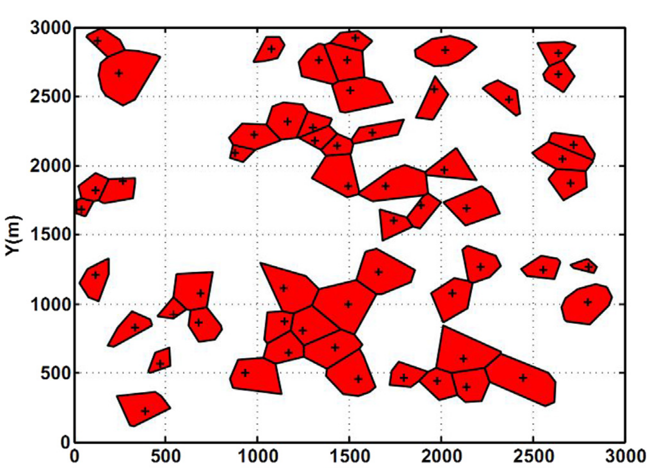

Fig. 3. Sample wind farm domain.

The main goal of our test cases is to investigate the effect of constraint severity on energy generation and noise production of wind farms. To this end, the wind farm domain is divided into 225 random polygons ($n_P = 225$) with areas of the same order of the magnitude. Based on industrial wind farm design experience, test cases with feasibility percentages (ϕ) of 70%, 80%, and 90% are generated. Fig. 3 depicts a sample wind farm test case with ϕ=80%, the noise receptors, represented with (+) in the figure, are placed randomly inside each non-feasible polygon. Thus, the more constrained the domain becomes, the more noise receptors it will have. The optimization is performed for 5, 10, and 15 identical turbines and, in order to account for GA's randomness, each optimization is carried out 5 times for each test case.

The population size and the number of generations for the GA were determined based on a set of computational experiments on sample test cases with the above mentioned land availabilities. Following Kwong et al. [11,10] populations with 100, 150, and 200 individuals were examined and the corresponding number of generations was determined such that the total number of objective function evaluations remained constant. A population size of 200 resulted in the best solutions for 70% feasible domains, regardless of the number of turbines in the wind farm. In a similar fashion, for 80% and 90% of land availabilities, the population sizes of 150 and 100 performed the best, respectively. It should be noted that the aforementioned population sizes are not necessarily the optimal population sizes, i.e., those which would guarantee the best performance of GA. The main goal here is to find a population size that has an acceptable performance for a given test case, and to use this population size consistently for our experiments. To this end, a small number of experiments was carried out to find population size and number of generations that result in the best performance for a given number of function evaluations. As a result, there might be several other GA parameters affecting the performance of a given population size that were not investigated in these experiments. Thus, the observed interplay between the percentage of land availability of the test case and the best-performing population size cannot be generalized to all wind farm problems, although the existence of this interplay is not unexpected considering that land availability is a measure of constraint severity, i.e., of the size of the search space. In any case, the investigation of optimal GA parameters for the constrained WFLO problem, though an interesting area to explore in the future, is beyond the scope of the present study.

Finally, it should be mentioned that all our tests were performed with an in-house C++ implementation of the NSGA-II algorithm with static, dynamic and death penalty modes, compiled with the TDM-GCC version 4.7.1 compiler under Linux Red Hat version 6.2. This code is run serially on a Dell PowerEdge T420 Tower Server with 2 Intel Xeon E5-2400 processors and 164 GB of RAM.

In the next section, the results of these tests are discussed in detail. First, we discuss how the choice of constraint handling approach affects the optimization results, in terms of the quality of the obtained solutions and the required computational effort. Second, the effect of constraint severity (feasibility percentage) and number of turbines on energy-noise trade-off is investigated. Finally, the impact of different spatial distributions of non-feasible areas, characterized by the proposed uniformity parameter (UP), is studied for a given feasibility percentage and number of turbines.

6. Results and discussion

As an introduction to the energy-noise trade-off discussion, it is advantageous to get an understanding about how the constraint severity can affect the solutions of the WFLO problem. For instance, the probability of finding a feasible layout by randomly placing

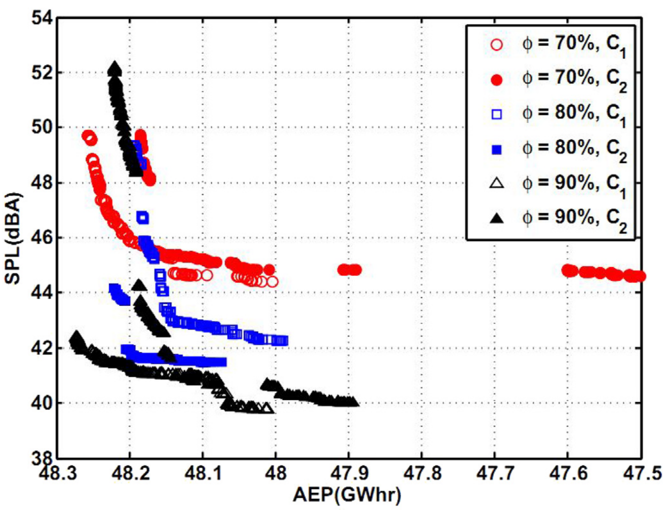

Fig. 4. Energy-noise trade-off attained by the dynamic penalty approach and 2 different penalty coefficients for 10 turbines. $C_1 = (t/n_{gen})^2 \times 10^4$ and $C_2 = (2t/n_{gen})^2 \times 10^4$.

5 turbines in a domain with 90% of land availability is $0.9^5 \times 100 = 59.05\%$. However, this probability decreases drastically to 16.81%, when placing 5 turbines randomly in a domain with 70% of land available. This reduction demonstrates that the probability of finding a feasible layout decreases exponentially with the number of turbines. More so, in industrial wind farms, where the number of turbines in a wind farm is usually more than 5 and it is not unusual to have land availabilities below 50%, the above mentioned probability decreases even further and makes finding feasible layouts more difficult for any stochastic optimization algorithm.

6.1. Performance of constraint handling approaches

With this brief introduction about the effect of constraint severity on the energy-noise trade-off, we now compare the performance of the constraint handling approaches in the context of constrained WFLO problem. As was stated before, to avoid convergence problems that may arise from inadequate penalization of infeasible solutions, the experiments were run with two different sets of penalty coefficients, C_1 and C_2, for both static and dynamic penalty approaches, with values as discussed in Section 4.2. The effect of using these sets of penalty coefficients on the results are shown in Fig. 4. The intersections and the overlaps of the Pareto sets attained by the first and the second sets of penalty coefficients for 10 turbines indicate that different sets of penalty coefficients have to be implemented in the context of the constrained WFLO problem to make the results reliable. Thus, the comparison of the constraint handling approaches is based on the best solutions attained by merging the solutions from different sets of penalty coefficients.

Table 2 presents the best performing constraint handling approaches in terms of solution quality, quantity, energy generation range and noise production range for each test case. A given solution (i.e. a given Pareto set) is considered to have a better quality if its maximum energy generation is higher and its minimum noise production is lower, i.e., if its dominated area in the objective space is larger. On the other hand, if the number (cardinality) of feasible/optimal layouts included in a solution (Pareto set) is larger, the solution is considered to have a better quantity. We also utilized two other metrics to characterize the distribution of the optimal layouts in the objective space. A solution is said to have better energy generation range if the difference of maximum and minimum energy generated by its layouts is larger. In a similar way, a

Table 2
Best performing constraint handling approaches with respect to solution quality, quantity, energy generation range, and noise generation range.

n_T	ϕ	Solution quality	Solution quantity	AEP range	SPL range
5	70%	Dynamic	Static	Static	Dynamic
5	80%	Dynamic	Static	Dynamic	Dynamic
5	90%	Dynamic	Static	Static	Dynamic
10	70%	Dynamic	Static	Dynamic	Dynamic
10	80%	Dynamic	Static	Static	Static
10	90%	Dynamic	Static	Static	Static
15	70%	Dynamic	Static	Dynamic	Static
15	80%	Dynamic	Static	Dynamic	Dynamic
15	90%	Dynamic	Static	Dynamic	Static

Pareto set is better in terms of noise production range, if the noise production of its layouts covers a wider range in the objective space. From Table 2, it can be noted that the dynamic penalty approach performs the best in terms of solution quality for all the test cases, presumably due to its balance between local and global searches. Regarding the quantity of solutions, the static penalty approach is capable of finding more feasible layouts for the test cases with 5 and 10 turbines. In these test cases, feasible layouts are found easier by random sampling as a result of the relatively small number of turbines. Thus, the static penalty approach, which favours domain exploration, seems to find more feasible layouts. By increasing the number of turbines to 15, finding feasible layouts becomes exponentially more difficult, as discussed before. Hence, the number of feasible/optimal layouts found by the dynamic penalty approach becomes very close to the cardinality of the Pareto set found by the static penalty function.

Regarding the computational performance of constraint handling methods, Table 3 shows the convergence and average run-time over 10 runs, i.e., 5 random runs with C_1 and 5 random runs with C_2, for 5, 10, and 15 turbines, and a domain feasibility of 80%. A set of preliminary runs with a termination criteria of 40,000 objective function evaluations (results not shown here) showed that the run-time associated with the death penalty is quite large (30.84 h for 5 turbines and 80% feasibility), due to the additional objective function evaluations that are required after discarding each infeasible layout. This deficiency, together with the poor performance of death penalty function on the preliminary results, persuaded us to not to use it for the final experiments with 80,000 objective function evaluations, shown in Table 3. As Table 3 shows, the run-time and convergence of the static and dynamic penalty approaches are rather close to each other. Even though the run-time associated with the dynamic approach is less than that of the static one for some cases, the dynamic penalty does not have a noticeable superiority over the static penalties in this aspect.

6.2. Effect of constraints on energy-noise trade-off

After investigating the performance of the constraint handling methods, we move on to discuss the effects of land use constraints

Table 3
Averaged Run-time (hr) and convergence (out of 10) for test cases with 80% feasibility and a maximum objective function evaluation of 80,000. Convergence is defined as meeting the convergence criteria, as opposed to terminating a run when the maximum number of evaluations is reached.

n_T	ϕ	Static penalty		Dynamic penalty	
		Run-time	Convergence	Run-time	Convergence
5	80%	19.75	8/10	18.86	9/10
10	80%	70.87	1/10	78.15	1/10
15	80%	149.75	0/10	149.53	0/10

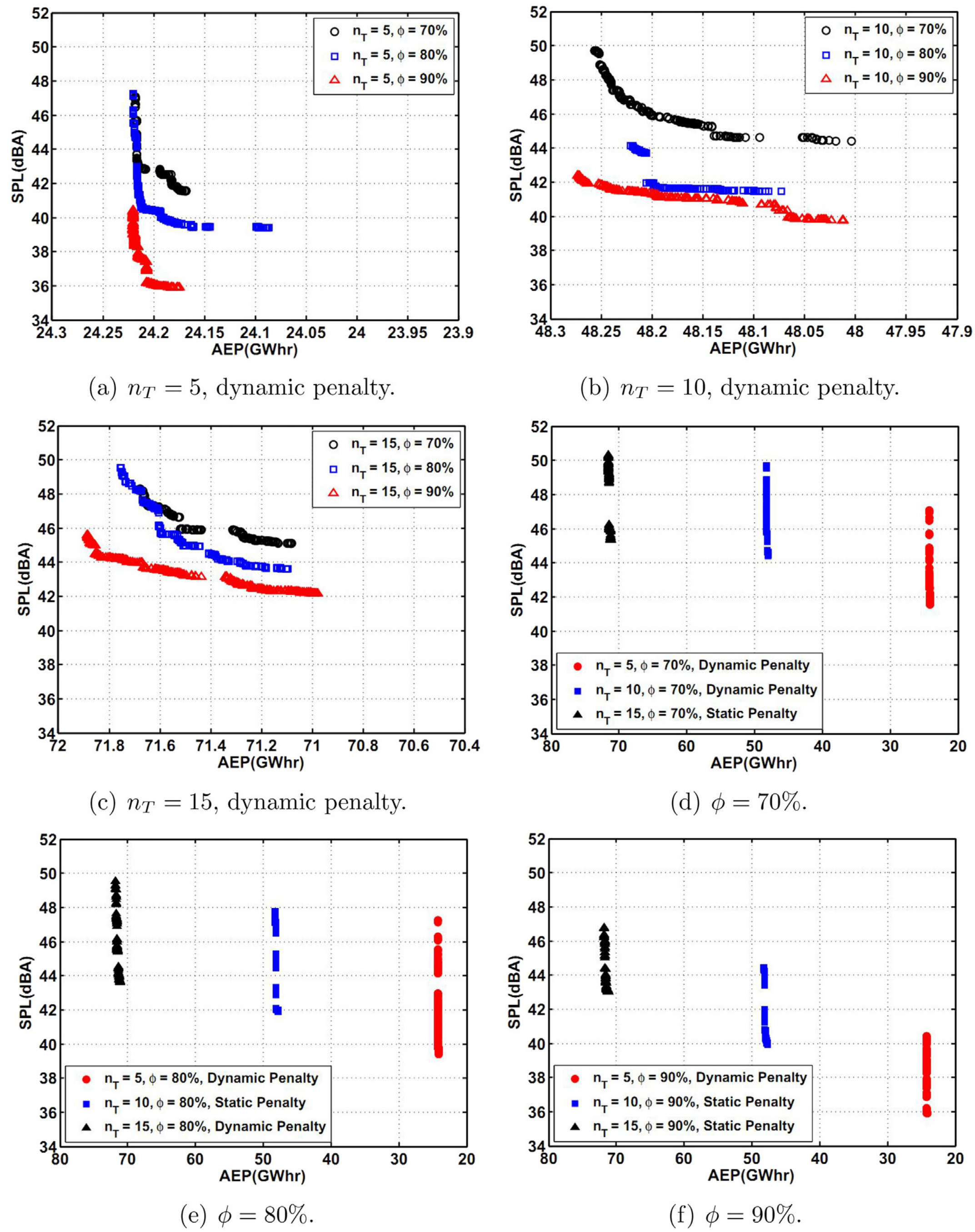

(a) $n_T = 5$, dynamic penalty. (b) $n_T = 10$, dynamic penalty.

(c) $n_T = 15$, dynamic penalty. (d) $\phi = 70\%$.

(e) $\phi = 80\%$. (f) $\phi = 90\%$.

Fig. 5. Energy-noise trade-off for different number of turbines and domain feasibilities.

on energy-noise trade-off. To achieve this goal, we base our discussion on the results with the best quality according to Table 2. Fig. 5(a–c), compare the energy-noise trade-off with different land availabilities, but with a specific number of turbines. It should be noted that the x axis in these figures is reversed, so that the utopia point, i.e., the infimum of the objective functions vector, is located in the bottom left corner of the figures. Also, each data point represents a layout and the Pareto front is the set of non-dominated data points. These figures show that as constraint severity increases, maximum energy generation decreases, while minimum attainable noise is increased. The most significant fact depicted by these figures is that the severity of land use constraints is more influential on noise production compared to energy generation. As the land use constraints become more severe, more noise receptors are located in the domain, making it more likely for the turbines to be placed close to them. More importantly, the proximity constraint protects turbines from the wake region of each other and does not let the regulatory constraint affect the energy generation to the same extent to which it affects the noise propagation.

The energy-noise trade-off is also investigated for different number of turbines and a given, fixed value of ϕ. Fig. 5(d–f) depict that for all the feasibility percentages both energy generation and minimum attainable noise are strongly dependent on the number of turbines. It should be noted that this comparison is carried out

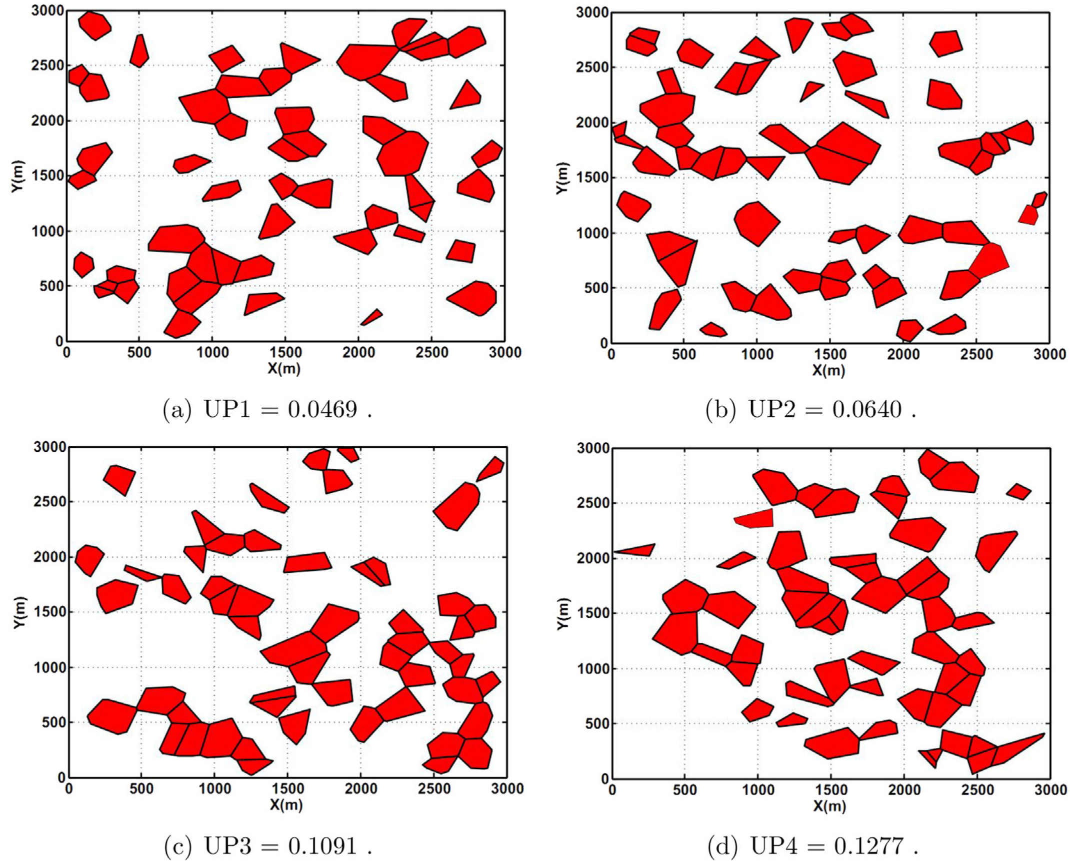

Fig. 6. Spatial distribution of non-feasible areas for four different values of the uniformity parameter (UP). Cases (a) to (d) have the same 80% land availability.

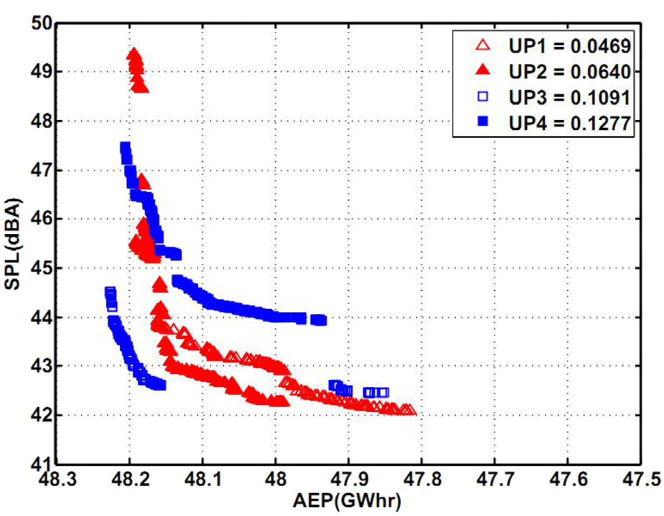

Fig. 7. Energy-noise trade-off for 10 turbines and 80% of land availability with different distribution uniformities of the non-feasible areas.

using the solutions with a wider range of noise production according to Table 2. As it is depicted by Fig. 5 and due to the proximity constraint, the noise production (SPL) has a wider range compared to energy generation (AEP).

The other parameter that can impact the results of the optimization is the spatial distribution uniformity of the non-feasible areas in the domain. To assess this effect, we created 4 test cases with 80% land availability and different uniformity parameters, optimizing the layout of 10 turbines. Fig. 6 shows the spatial distribution of non-feasible areas for these test cases. The results for these domains, obtained with the dynamic penalty approach, are depicted in Fig. 7. According to Fig. 7, domains 3 and 4 produce better solutions in terms of quantity; however, the objective functions' ranges of the feasible/optimal layouts found in these two domains are relatively small compared to that of the other domains, presumably because the uneven distribution of non-feasible areas increases the probability of having large, continuous portions of feasible land. Thus, GA explores this feasible area extensively and finds a large number of layouts that have similar energy generation and noise production, but are not necessarily optimal. On the other hand, with smaller UP s, locating turbines between the narrow spacings of the evenly distributed non-feasible areas becomes difficult; thus the cardinality of the feasible layouts found by the GA decreases. An additional observation is that, for lower values of UP (more uniformly distributed non-feasible areas), the turbine layouts obtained (not shown here) are more dissimilar from each other, and they result in larger ranges of energy generation and noise production (shown in red triangles in Fig. 7) than test cases with higher UP (shown in blue squares in Fig. 7). Finally, it should be noted that UP calculates the distribution uniformity with respect to the centers of the non-feasible polygons and does not consider their areas. As such, we consider UP and incomplete characterization of the spatial distribution uniformity of the non-feasible areas in the domain. In our ongoing work, we continue to evaluate approaches to characterize the complexity of a WFLO problem case based on the severity and spatial distribution of land use constraints.

7. Concluding remarks

This paper studied a multi-objective energy-noise wind farm layout optimization problem including land-use and proximity constraints. The optimization was carried out with the NSGA-II evolutionary algorithm and the constraints were handled using static, dynamic, and death penalty functions. The energy-noise trade-off was studied for different levels of constraint severity, numbers of turbines, and distribution uniformity of the non-feasible areas within the wind farm domain. In using the penalty functions, we conducted our constraint handling based on different degrees of objective function penalization.

The main purpose of this work was to characterize the impact of the land-use constraints on the energy-noise trade-off. It is shown that a smaller percentage of land availability causes a decrease in energy generation and increases the effective noise level at the receptors. However, the most interesting finding in this area was that changes in the severity of land use constraints do not affect the energy generation to the same extent that they affect noise propagation, because of the dampening effect of the turbine proximity constraint. It should also be noted that the increase in the number of turbines results in an increase in both energy generation and noise production.

Regarding the use of constraint handling methods, we observed that the extensive global search of the static and death penalty approaches result in finding more feasible layouts. However, as the number of turbines is increased and the domain becomes more crowded, static and death penalty approaches are more likely to converge to sub-optimal layouts. In contrast, the dynamic penalty approach converges to layouts with more energy generation and less noise production compared to the other methods. Furthermore, our experiments on the domains with higher turbine densities (number of turbines per km^2) showed that the dynamic penalty method finds at least as many feasible optimal layouts as the other penalization approaches.

This study also investigated the impact of the distribution uniformity of the non-feasible areas on the energy-noise trade-off. The proposed uniformity metric characterizes the spatial distribution of the non-feasible areas based on their geometrical center. According to our results, a non-uniform distribution of the non-feasible areas leads to finding more feasible/optimal layouts. However, it is observed that these solutions have relatively small energy generation and noise production ranges.

For future studies, we will focus on devising a uniformity distribution metric that considers both the geometrical centers and the sizes (areas) of the non-feasible land portions, and on documenting the energy-noise trade-off for the test cases with larger numbers of turbines on a given terrain area, i.e. larger turbine densities. For this purpose, alternative optimization algorithms, or parallelized versions of our current algorithms will be explored for better computational efficiency. In addition, the inclusion of a comprehensive cost model that includes land prices, energy prices, participation incentives for landowners, government incentives, among others, has the potential to enrich the discussion in the context of wind farm economics and government policy.

Acknowledgment

This work was supported by the Natural Sciences and Engineering Research Council of Canada (NSERC), through the Collaborative Research and Development (CRD) and Discovery Grant programs. The authors would like to thank Hatch Ltd. for its financial support of this research. M. D. Gu would like to acknowledge support from the NSERC Undergraduate Summer Research Awards (USRA) program.

References

[1] International Energy Association (IEA) Wind, 2012 Annual Report, IEA Wind, 2013.
[2] Global Wind Energy Council (GWEC), Global Wind Report: Annual Market Update 2013, GWEC, 2014.
[3] European Wind Energy Association (EWEA), EWEA 2013 Annual Report: Building a Stable Future, EWEA, 2014.
[4] Chief Medical Officer of Health (CMOH) of Ontario, The Potential Health Impact of Wind Turbines, Technical Report, Ministry of Health and Long-term Care, Government of Canada, 2010.
[5] Ministry of the Environment (Canada), Compliance Protocol for Wind Turbine Noise - Guideline for Acoustic Assessment and Measurement, Technical Report, Ministry of the Environment (Canada), 2011.
[6] Ministry of the Environment (Canada), Noise Guidelines for Wind Farms, Technical Report, 2008.
[7] R. Saidur, N. Rahim, M. Islam, K. Solangi, Environmental impact of wind energy, Renew. Sustain. Energy Rev. 15 (2011) 2423–2430.
[8] G. Mosetti, C. Poloni, B. Diviacco, Optimization of wind turbine positioning in large windfarms by means of a genetic algorithm, J. Wind Eng. Industrial Aerodynamics 51 (1994) 105–116.
[9] S. Grady, M. Hussaini, M.M. Abdullah, Placement of wind turbines using genetic algorithms, Renew. Energy 30 (2005) 259–270.
[10] W.Y. Kwong, P.Y. Zhang, D.A. Romero, J. Moran, M. Morgenroth, C.H. Amon, Wind farm layout optimization considering energy generation and noise propagation, in: Proc. International Design Engineering Technical Conferences & Computers and Information in Engineering Conference (IDETC/CIE), 2012, pp. 1–10.
[11] W.Y. Kwong, P.Y. Zhang, D.A. Romero, J. Moran, M. Morgenroth, C.H. Amon, Multi-objective wind farm layout optimization considering energy generation and noise propagation with NSGA-II, J. Mech. Des. 136 (2014) 091010–091011.
[12] J.H. Holland, Adaptation in Natural and Artificial Systems: an Introductory Analysis with Applications to Biology, Control, and Artificial Intelligence, University of Michigan Press, 1975.
[13] K. Deb, A. Pratap, S. Agarwal, T. Meyarivan, A fast and elitist multiobjective genetic algorithm: NSGA-II, Evolutionary Computation, IEEE Trans. 6 (2002) 182–197.
[14] C.A. Coello Coello, Theoretical and numerical constraint-handling techniques used with evolutionary algorithms: a survey of the state of the art, Comput. methods Appl. Mech. Eng. 191 (2002) 1245–1287.
[15] J. Kennedy, Particle swarm optimization, in: Encyclopedia of Machine Learning, Springer, 2010, pp. 760–766.
[16] C. Wan, J. Wang, G. Yang, X. Zhang, Optimal micro-siting of wind farms by particle swarm optimization, in: Advances in Swarm Intelligence, Springer, 2010, pp. 198–205.
[17] M. Bilbao, E. Alba, Simulated annealing for optimization of wind farm annual profit, in: Logistics and Industrial Informatics, 2009. LINDI 2009. 2nd International, IEEE, 2009, pp. 1–5.
[18] B.L. Du Pont, J. Cagan, An extended pattern search approach to wind farm layout optimization, J. Mech. Des. 134 (2012) 081002.
[19] S. Şişbot, Ö. Turgut, M. Tunç, Ü. Çamdalı, Optimal positioning of wind turbines on Gökçeada using multi-objective genetic algorithm, Wind Energy 13 (2010) 297–306.
[20] A. Kusiak, Z. Song, Design of wind farm layout for maximum wind energy capture, Renew. Energy 35 (2010) 685–694.
[21] P.-E. Réthoré, P. Fuglsang, G.C. Larsen, T. Buhl, T.J. Larsen, H.A. Madsen, TopFarm: multi-fidelity optimization of offshore wind farm, in: Proceedings of the Twenty-first International Offshore and Polar Engineering Conference, International Society of Offshore and Polar Engineers, 2011, pp. 516–524.
[22] B. Saavedra Moreno, S. Salcedo Sanz, A. Paniagua Tineo, L. Prieto, A. Portilla Figueras, Seeding evolutionary algorithms with heuristics for optimal wind turbines positioning in wind farms, Renew. Energy 36 (2011) 2838–2844.
[23] J.S. González, A.G. Gonzalez Rodriguez, J.C. Mora, J.R. Santos, M.B. Payan, Optimization of wind farm turbines layout using an evolutive algorithm, Renew. Energy 35 (2010) 1671–1681.
[24] J.S. Gonzalez, M. Burgos Payan, J.M. Riquelme-Santos, Optimization of wind farm turbine layout including decision making under risk, Syst. J. IEEE 6 (2012) 94–102.
[25] S. Chowdhury, J. Zhang, A. Messac, L. Castillo, Characterizing the influence of land configuration on the optimal wind farm performance, in: ASME 2011 International Design Engineering Technical Conferences & Computers and Information in Engineering Conference (IDETC/CIE 2011), No. DETC2011–48731, ASME, 2011.
[26] S. Chowdhury, J. Zhang, A. Messac, L. Castillo, Unrestricted wind farm layout optimization (UWFLO): investigating key factors influencing the maximum power generation, Renew. Energy 38 (2012) 16–30.
[27] S. Chowdhury, J. Zhang, A. Messac, L. Castillo, Optimizing the arrangement and the selection of turbines for wind farms subject to varying wind conditions, Renew. Energy 52 (2013) 273–282.

[28] S. Donovan, G. Nates, H. Waterer, R. Archer, Mixed integer programming models for wind farm design, in: Slides Used at MIP 2008 Workshop on Mixed Integer Programming, Columbia University, New York City, 2008.
[29] S. Donovan, An improved mixed integer programming model for wind farm layout optimisation, in: Proceedings of the 41th Annual Conference of the Operations Research Society, Wellington, New Zealand, 2006.
[30] P. Fagerfjäll, Optimizing Wind Farm Layout: More Bang for the Buck Using Mixed Integer Linear Programming, Chalmers University of Technology and Gothenburg University, 2010.
[31] R. Archer, G. Nates, S. Donovan, H. Waterer, Wind turbine interference in a wind farm layout optimization mixed integer linear programming model, Wind Eng. 35 (2011) 165–175.
[32] S. Turner, D.A. Romero, P.Y. Zhang, C.H. Amon, T.C.Y. Chan, A new mathematical programming approach to optimize wind farm layouts, Renew. Energy 63 (2014) 674–680.
[33] P.Y. Zhang, D.A. Romero, J.C. Beck, C.H. Amon, Solving wind farm layout optimization with mixed integer programming and constraint programming, in: Integration of AI and OR Techniques in Constraint Programming for Combinatorial Optimization Problems, Springer, 2013, pp. 284–299.
[34] L. Chen, E. MacDonald, A system-level cost-of-energy wind farm layout optimization with landowner modeling, Energy Convers. Manag. 77 (2014) 484–494.
[35] C.M. Fonseca, P.J. Fleming, Multiobjective optimization and multiple constraint handling with evolutionary algorithms. I. A unified formulation, systems, man and cybernetics, part a: systems and humans, IEEE Trans. 28 (1998) 26–37.
[36] T. Ray, K. Tai, K.C. Seow, Multiobjective design optimization by an evolutionary algorithm, Eng. Optim. 33 (2001) 399–424.
[37] S. Yamani Douzi Sorkhabi, D.A. Romero, G.K. Yan, M.D. Gu, J. Moran, M. Morgenroth, C.H. Amon, Multi-objective energy-noise wind farm layout optimization under land use constraints, in: ASME 2014 International Mechanical Engineering Congress and Exposition, American Society of Mechanical Engineers, 2014.
[38] N.O. Jensen, A Note on Wind Generator Interaction, 1983.
[39] J. Manwell, J. McGowan, A. Rogers, Aerodynamics of Wind Turbines, Wind Energy Explained: Theory, Design and Application, Second ed., 2009, pp. 91–155.
[40] ISO 9613–2:1996, Acoustics - Attenuation of Sound during Propagation Outdoors - Part 2: General Method of Calculation (ISO 9613-2:1996), ISO, Geneva, Switzerland, 1996.
[41] D. Zwillinger, CRC Standard Mathematical Tables and Formulae, CRC press, 1987.
[42] X. Gandibleux, Metaheuristics for Multiobjective Optimisation, volume 535, Springer, 2004.
[43] J.A. Joines, C.R. Houck, On the use of non-stationary penalty functions to solve nonlinear constrained optimization problems with GA's, in: evolutionary Computation, 1994, in: IEEE World Congress on Computational Intelligence., Proceedings of the First IEEE Conference on, IEEE, 1994, pp. 579–584.
[44] A. Homaifar, C.X. Qi, S.H. Lai, Constrained optimization via genetic algorithms, Simulation 62 (1994) 242–253.
[45] A. Smith, A.E. Smith, D.W. Coit, Penalty functions, in: T. Baeck, D. Fogel, Z. Michalewicz (Eds.), Handbook of Evolutionary Computation, IOP Publishing Ltd, 1997.
[46] S. Kazarlis, V. Petridis, Varying fitness functions in genetic algorithms: studying the rate of increase of the dynamic penalty terms, in: Parallel Problem Solving from NaturePPSN V, Springer, 1998, pp. 211–220.
[47] H. Weyl, Über die Gleichverteilung von Zahlen mod. eins, Math. Ann. 77 (1916) 313–352.
[48] F. Hickernell, A generalized discrepancy and quadrature error bound, Math. Comput. Am. Math. Soc. 67 (1998) 299–322.
[49] K.-T. Fang, R. Li, A. Sudjianto, Design and Modeling for Computer Experiments, CRC Press, 2010.